Neutron Capture Cross Section Measurement of Pr in the Energy Region from 0.003 eV to 140 keV by Linac Time-of-Flight Method

Samyol Lee [a], Shuji Yamamoto [a], Katsuhei Kobayashi [a], Jungran Yoon [b], and Taeik Ro [b]

[a] *Research Reactor Institute, Kyoto University, Kumatori-cho, Sennan-gun, Osaka, 590-0494, Japan*

koba@rri.kyoto-u.ac.jp

[b] *Dong-A University, 840 Hadan 2-dong, Saha-gu, Pusan, 604-714, Korea*

The cross section of the Pr(n,γ) reaction has been measured in the energy region from 0.003 eV to 140 keV by the neutron time-of-flight (TOF) method with a 46-MeV electron linear accelerator (linac) of the Research Reactor Institute, Kyoto University (KURRI). An assembly of $Bi_4Ge_3O_{12}$ (BGO) scintillators was employed as a total energy absorption detector for the prompt capture γ-ray measurement from the sample. In order to determine the neutron flux impinging on the capture sample, a plug of ^{10}B powder sample was used. The measured result was compared with the previous experimental and the evaluated data.

1. Introduction

Praseodymium-141 (^{141}Pr) is a kind of fission products (FPs) which are produced in Light Water Reactors (LWRs) and Liquid-Metal-Cooled Fast Breeders Reactors (LMFBRs). The cumulative fission yields of the thermal neutron-induced fission of ^{235}U is 5.8 %[1]. The yield value is pretty large in the fission products and ^{141}Pr may be apt to accumulate in the spent-fuels. Therefore, accurate measurement of the nuclear data, especially the neutron capture cross section, is necessary for the assessment of reactor safety and for the investigation of high-burn-up core characteristics[2,3]. According to the evaluated data in ENDF/B-VI[4], the capture cross sections in the thermal and the keV energy regions are 11.5 and about 0.1 b, respectively. Since the ^{141}Pr nuclide has the neutron magic number (N=82) and excess proton on the $2d_{5/2}$ sub-shell, the capture cross section may not be so large as expected. However, the accurate nuclear data of ^{141}Pr is thought to be needed for evaluating the nuclear-transmutation performance in reactors. In the keV energy region, moreover, the capture cross section is also important for the study on the s-process for nucleosynthesis in stars.[5,6,7]

Although the energy dependent cross section for the ^{141}Pr(n,γ) reaction has been measured before, no data has been experimentally obtained below 22 eV, except for the thermal neutron capture cross section. Konks et al.[8] measured the cross section at energies from 22 eV to 40 keV with a lead slowing-down spectrometer, which gave poor energy resolution of about 30 to 35 % at full-width at half-maximum (FWHM). Gibbons et al.[9] obtained the data in the energy range of 7 to 170 keV using a Van de Graaff accelerator and a liquid scintillation tank detector. Taylor et al.[10] measured the cross section between 3 and 200 keV by the neutron time-of-flight (TOF) method using an electron linear accelerator (linac) and a pair of non-hydrogenous liquid scintillators. Very recently, the experimental group of Igashira et al.[11] measured the capture cross sections at energies of 10 to 100 keV making use of a 3-MV Pelletron accelerator and a large anti-Compton NaI(Tl) γ–ray spectrometer. The capture cross section has been compiled in JENDL-3.2[12], ENDF/B-VI[4], and JEF-2.2[13].

As mentioned above, the current situation of the experimental data is not always satisfied in quality and quantity. In the current study, the relative energy dependent cross section of the ^{141}Pr(n,γ) reaction has been measured by the neutron time-of-flight (TOF) method with a 46-MeV electron linear accelerator (linac) of the Research Reactor Institute, Kyoto University (KURRI). Twelve pieces of $Bi_4Ge_3O_{12}$ (BGO) scintillators were employed to measure capture gamma-rays from the sample as a total energy absorption detector[14]. The energy dependent neutron flux was obtained with the boron-10 (^{10}B) sample and the ^{10}B(n,$\alpha\gamma$) standard cross section. The result has been normalized to the thermal neutron capture cross section value of ENDF/B-VI data, and the result has been compared with the previous experimental data and the evaluated cross sections in JENDL-3.2, ENDF/B-VI, and JEF-2.2.

2. Experimental procedure

The experimental arrangement is shown in **Fig. 1**. Bursts of fast neutrons were produced from the water-cooled photoneutron target, which was made of twelve sheets of Ta plate, 5 cm in diameter and the effective thickness is ~3 cm[15]. This target was set at the center of a water tank, 30 cm in diameter and 35 cm high with wall thickness of 0.8 cm, to moderate the pulsed fast neutrons. A Pb block, 5 cm × 5 cm and 10 cm long, was placed in front of the Ta target to reduce the γ-flash generated by the electron burst from the target. The capture sample was placed at a distance of 12.7±0.02 m from the Ta target. The neutron and γ-ray collimation system was mainly composed of B_4C, Pb, Li_2CO_3 and borated paraffin, and tapered from ~12 cm in diameter at the entrance of the flight tube to 1.8 cm at the BGO assembly. In the experiment above 1 eV, a Cd sheet of 0.5 mm in thickness has placed in the neutron beam to suppress overlap of thermal neutrons from the previous pulses due to the high frequency operation.

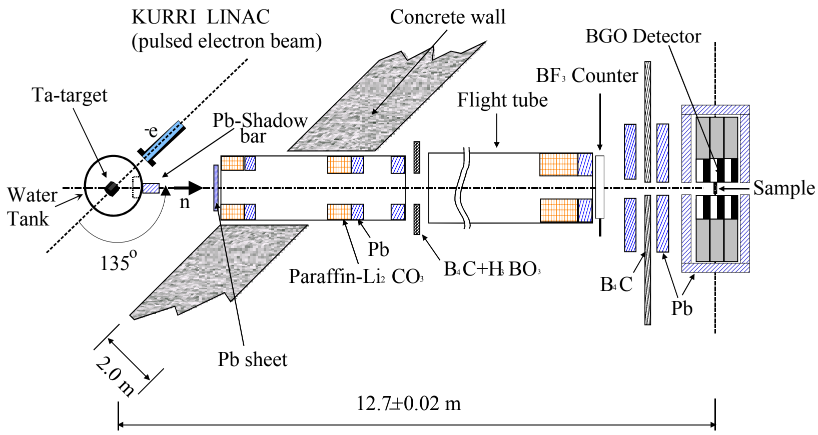

Fig. 1. Experimental arrangement for the capture cross section measurement.

In the background measurement, we measured the γ-ray from the blank sample (without Pr sample). The neutron beam intensity during the measurement was monitored with a BF_3 counter inserted into the neutron beam. The linac was operated with two different modes; One is for that below 20 eV with the repetition rate of 50 Hz, the pulse width of 3.0 μs, the peak current of 0.5 A, and the electron energy of ~30 MeV. The other is for that above 1 eV with the repetition rate of 300 Hz, the pulse width of 0.010 μs, the peak current of 6 A, and the electron energy of ~30 MeV, respectively.

In the measurement, we have employed three kinds of sample, as shown in **Table 1**. We have paid attention to the sample thickness of Pr not to be so large for the multiple-scattering and self-shielding corrections in the sample. The ^{10}B sample in the form of powder packed in a thin aluminum case was used to measure the relative neutron flux. The graphite sample was also utilized for the experimental investigation of background due to neutrons scattered by the Pr sample. Because although the inside of the through-hole in the BGO assembly was covered with ^6LiF tiles of 3 mm in thickness to absorb neutrons scattered by the capture sample, the tiles were not always enough to shield against higher energy neutrons above 10 eV[14]. The background to the scattered neutrons were corrected by considering the graphite thickness equivalent to the scattering cross section of the capture sample.

The BGO assembly, which is used for the capture γ-ray spectrometer, consists of twelve scintillation bricks of 5 × 5 × 7.5 cm^3, and the total volume of the BGO scintillators is 2.25 liters[14]. Each BGO scintillators is equipped with a photo-multiplier tube of 3.8 cm in diameter. A through-hole of 1.8 × 1.8 cm^2 in section is made in the BGO assembly. A collimated neutron beam is led through the hole to the capture sample that is placed at the center of the BGO assembly. Moreover, the BGO assembly installed in a house made of lead bricks of 5 to 10 cm in thickness to shield against background radiation from the surroundings.

Two kinds of signals were stored in the FAST ComTec's MPA/PC-multi-parameter system linked to a personal computer. One is for the capture event measurement from the BGO detection system, and the other is for the BF_3 counter to monitor the neutron beam intensity among the experimental runs. Output signals from the BGO detection system were fed into the time digitizer, which was initiated by the electron burst through the fast amplifier and the discriminator, and were stored in the multi-channel analyzer. The signals from the BF_3 counter were also fed into the time digitizer through the linear amplifier and the timing-single channel analyzer. The data obtained were all stored in the multi-parameter system.

Table 1. Physical parameters of the samples used in the current measurements.

Sample	Physical form	Purity (%)	Isotopic Composition (%)	Thickness		Size
				(g/cm^2)	(mm)	—
^{141}Pr	Foil	99.9	100	1.609	3.0	1.27 cm in diam.
^{10}B$^{\dagger 1}$	^{10}B Powder	99.999	^{10}B: 96.98 ^{11}B: 3.02	0.872	8.0	1.8 × 1.8 cm^2
Graphite	Plate	99.99	100	1.892	10.0	1.8 × 1.8 cm^2

†1 Each sample (powder) was packed into a thin aluminum case (0.1 mm in thickness).

3. Data processing

3.1. Derivation of the neutron capture cross section

A ^{10}B sample was used to determine the incident neutron flux on the sample. Since the thermal neutron cross section of the ^{10}B(n,$\alpha\gamma$) reaction is 3837±9 b[16], the ^{10}B sample (0.872 g/cm^2) is black for neutrons below several hundreds of keV as well as thermal neutrons. In addition, the energy dependent cross section ratio $^{10}\mathrm{B(n,}\alpha\gamma) / \{^{10}\mathrm{B(n,}\alpha\gamma)+^{10}\mathrm{B(n,}\alpha)\}$ is almost constant in the relevant energy region[17]. Then, the capture counting rate of the ^{10}B sample at energy $E, C_B(E)$, is given by the following relation:

$$C_B(E) = \varepsilon_B Y_B(E)\phi(E) = \varepsilon_B \phi(E), \tag{1}$$

where the subscript "*B*" means ^{10}B. $Y_B(E)$ is the capture yield and unity in the relevant energy, because the ^{10}B sample can be black. ε_B is the detection efficiency for the ^{10}B(n, $\alpha\gamma$) reaction. The neutron flux $\phi(E)$ at a certain energy *E* can be obtained from the following relation:

$$\phi(E) = C_B(E)/\varepsilon_B/Y_B(E). \tag{2}$$

The capture counting rate for the ^{141}Pr sample at energy $E, C_{Pr}(E)$, can be obtained from the following relation :

$$C_{Pr}(E) = \varepsilon_{Pr} Y_{Pr}(E)\phi(E), \tag{3}$$

where the subscript "*Pr*" means the sample of ^{141}Pr. Since the BGO detection system is a total energy absorption detector, the detection efficiency ε_{Pr} may be independent of neutron energy *E*. Finally, the capture yield $Y_{Pr}(E)$ can be obtained using Eqs. (2) and (3) as

$$Y_{Pr}(E) = \varepsilon \frac{C_{Pr}(E)}{C_B(E)} Y_B(E), \tag{4}$$

where ε is a relative detection efficiency obtained from $\varepsilon_B / \varepsilon_{Pr}$. In the case of the ^{10}B sample used in the current measurement, the capture yield $Y_B(E)$ is unity in the relevant energy region, as mentioned above.

4. Corrections and uncertainties

The capture yield, $Y(E)$ is a primary value to be determined from the number of capture events occurring in the sample. The neutron capture yield for the sample is given by[18]

$$Y(E) = \{1 - \exp(-N\sigma_t(E)t)\}\frac{\sigma_C(E)}{f_C(E)\sigma_t(E)}, \tag{5}$$

where N is the atomic density of the sample, $\sigma_t(E)$ is the neutron total cross section, t is the sample thickness, $\sigma_C(E)$ is the neutron capture cross section, and $f_C(E)$ is the correction function for the neutron scattering and/or self-shielding in the sample. Instead of the calculation with Eq. (5), we have employed the Monte Carlo code MCNP[19] and the cross sections in JENDL-3.2 to perform the detailed calculations considering the neutron transport in the sample. In the calculation, we have assumed that the capture sample is irradiated by the collimated parallel neutron beam. The random history number of the Monte Carlo calculation was 5,000,000. The correction function for the ^{10}B sample has been calculated by using Eq. (5), because the ^{10}B(n,$\alpha\gamma$) cross section has no resonance structure in the relevant energy region. After the neutron scattering and/or self-shielding correction, the capture cross section was derived in the low energy region of 0.003 to 20 eV. The result obtained was normalized to the reference thermal neutron cross section value at 0.0253 eV. For the high energy experiment in the energy range of 0.7 eV to 140 keV, the cross section was normalized to that in the low energy region by integrating the respective data in the overlapped energy region from 0.7 to 3 eV, after the correction.

The experimental uncertainties for the current measurement are 4.3 to 220 %, which are mainly due to the statistical errors (1.1 ~ 220 %) and uncertainties in the deviation of the ^{10}B(n,$\alpha\gamma$) cross section curve (2.4 %) and the reference cross section value (3.0 %). We had poor counting statistics in the cross section minimum energy region between the resonance peaks. The uncertainty of the γ-ray detection efficiency for the BGO assembly is about 0.45 %[20]. In addition, we have considered the uncertainties due to the background subtraction of about 1 % and the corrections for neutron self-shielding and/or neutron scattering effects of 1.3 %.

5. Results

The neutron capture cross section of ^{141}Pr has been measured from 0.003 eV to 140 keV by the linac TOF method and the result has been normalized at 0.0253 eV to the reference value (11.6±0.35 b), which was obtained very recently by Yoon et al[21].

The previous measurements and the evaluated data of JENDL-3.2[12], ENDF/B-VI[4] and JEF-2.2[13] are shown in **Fig. 2**. Most of the cross sections have been measured at energies more than keV. In the lower energy range, no experimental data has been reported before except for the thermal neutron cross sections and the data obtained by Konks et al.[8]. The data of Konks et al. are energy-broadened by the lead slowing-down spectrometer at the major resonance peak region. The data by Konks et al. are lower by about 18 % in average at energies from 1 to 40 keV, although their data tend to be in agreement with the current measurement from 5 to 40 keV within the experimental error. The data obtained by Taylor et al.[10] are in good agreement with the current measurement within the uncertainty. Very recently, the data by Harnood et al.[11] are in better agreement with the current result in the energy region from 12 to 70 keV. The data by Gibbons et al.[9] are in good agreement with the measurement and higher by 3.5 % in the energy region from 11.5 to 140 keV than the current measurement. We have observed a small resonance peak at about 5 eV. The peak structure has been also found in the neutron total cross section measurements[22,23]. Their results may support that there exists the small peak which we have observed at about 5 eV for the first time in the capture cross section measurement.

The evaluated data of JENDL-3.2, ENDF/B-VI and JEF-2.2 show general agreement with the current measurement in the relevant energy region. However, in the cross section minimum region of about 10 to 500 eV, the evaluated data of JENDL-3.2 and JEF-2.2 are considerably lower than the measurement, although the ENDF/B-VI is in good agreement within the error.

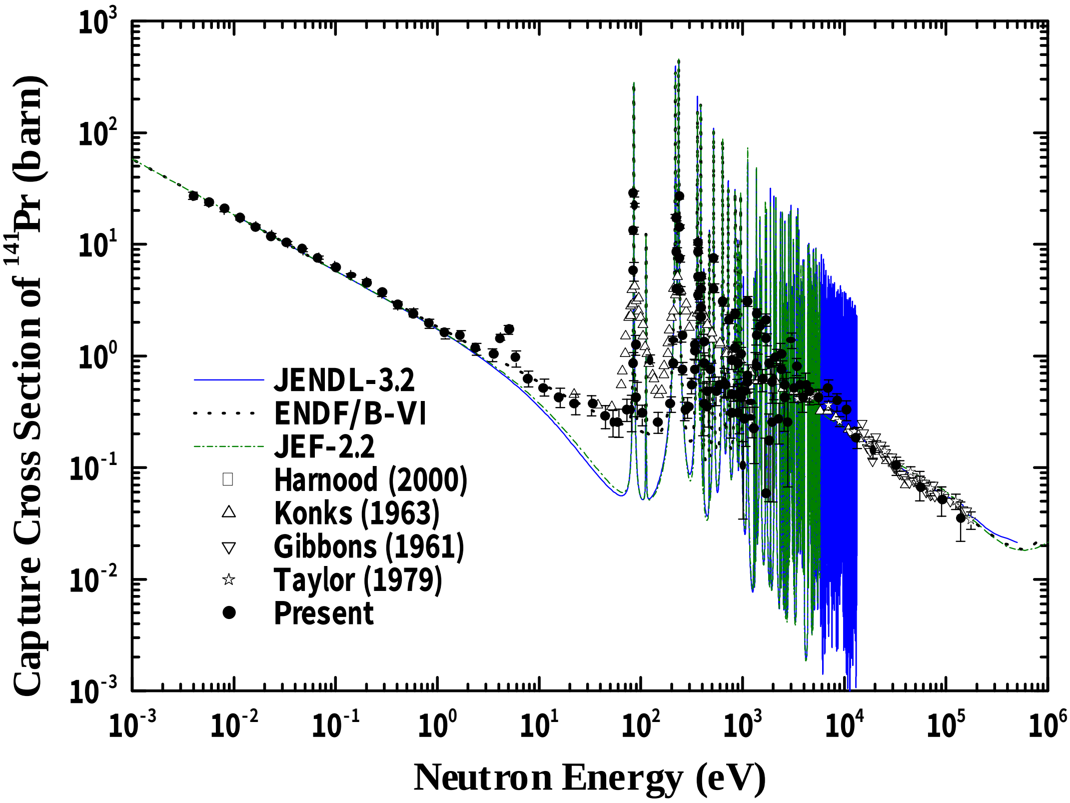

Fig. 2. Comparison of the previous experimental data and the evaluated cross sections with the present measurement for the Pr(n,γ) reaction.

6. Conclusion

The relative measurement of the ^{141}Pr(n,γ) cross section has been performed from 0.003 eV to 140 keV, and the result has been normalized at 0.0253 eV to the reference value (11.6±0.35 b), which was obtained very recently by Yoon et al[21]. The previous measurements and the evaluated data from ENDF/B-VI, JENDL-3.2 and JEF-2.2 are compared with the current measurement in **Fig. 2**. No experimental data have been reported before below 22 eV except for the thermal neutron cross section. As can be seen in **Fig. 2**, we have observed a small resonance peak at about 5 eV, whose peak structure has been found in the neutron total cross section measurements[22,23]. This fact may support the existence of the small resonance peak in the capture cross section curve. The data by Konks et al. have been measured with the lead slowing-down spectrometer[8]. In the non-resolved region from 5 to 40 keV, their data are close to the current measurement. The data by Gibbons et al.[9] and Taylor et al.[10] are in good agreement with the measurement. Very recently Harnood et al.[11] measured the cross section, which agreed well with the measurement at energies from 12 to 70 keV. The evaluated data from ENDF/B-VI, JENDL-3.2 and JEF-2.2 show good agreement with the current measurement in the relevant energy region, although the JENDL-3.2 and the JEF-2.2 data are considerably lower than the measurement and the ENDF/B-VI data in the cross section minimum region from 10 to 500 eV.

Acknowledgment

The authors would like to express their thanks to the linac staff of the Research Reactor Institute, Kyoto University (KURRI) for making it possible to operate the accelerator steadily. One of the authors (Samyol Lee) performed this study by the Grant-in-Aid (No.: 02122) for Scientific Research (Tokubetsu Kenkyuin Shorei-hi) of Japan Society for the Promotion of Science. A part of this study was supported by the Grant-in-Aid (No.: 13680588) for Scientific Research from the Ministry of Education, Culture, Sports, Science and Technology of Japan.

References

[1] H. Ihara (Ed.), JAERI-M 89-204 Tables and Figures from JNDC Nuclear Data Library of Fission Products Version 2 (1989) 157.
[2] R. L. Macklin and J. Halperin, Nucl. Sci. Eng. 73 (1980) 174.
[3] S. Mizuno, M. Igashira, and K. Masuda, J. Nucl. Sci. Tec. 36 (1999) 493.
[4] "ENDF-201, ENDF/B-VI Summary Documentation", BNL-NCS-17541, MOD1 New Evaluation (ENDF/B-VI) 4^{th} ed., P. F. ROSE, Ed., Brookhaven National Laboratory (1991); see also V. McLane and Members of The Cross Section Working Group "ENDF-201 ENDF/B-VI Summary Documentation Supplement 1 ENDF/HE-VI Summary Documentation", BNL NCS-17541, MOD3 Rev. 2 (ENDF/B-VI), Suppl. 1, 4^{th} ed., Brookhaven National Laboratory (1996).
[5] D. D. Clayton, "Principles of stellar evolution and nucleosynthesis", Univ. of Chicago Press, Chicago (1968).
[6] M. Busso and R. Gallino, Nucl. Phys. A621 (1997) 431c.
[7] C. Arlandini, M. Heil, R. Reifarth, F. Käppeler, and P. V. Sedyshev, Nucl. Phys. A688 (2001) 487c.
[8] V. A. Konks, Yu. P. PoPov, and F. L. Shapiro, Soviet Phys. JETP 19 (1964) 59.
[9] J. H. Gibbons, R. L. Macklin, P. D. Miller, and J. H. Neiler, Phys. Rev. 122 (1961) 182.
[10] R.B. Taylor, B. J. Allen, A. R. Del. Musgrove, and R. L. Macklin, Aus. J. Phys. 32 (1979) 551.
[11] S. Harnood, M. Igashira, T. Matsumoto, S. Mizuno, and T. Ohsaki, J. Nucl. Sci. Tech. 37 (2000) 740.
[12] "Descriptive Data of JENDL-3.2", JAERI-Data/ Code 98-006 (part II), K. Shibata, and T. Narita, Eds., Japan Atomic Energy Research Institute (1998).
[13] C. Nordborg, and M. Salvatores, "Status of the JEF Evaluated Data Library", Proc. Intl. Conf. Nuclear Data for Science and Technology, Gatlinberg, Tennessee, May 9-13, Vol. 2, p. 680, American Nuclear Society (1994).
[14] S. Yamamoto, K. Kobayashi, and Y. Fujita, J. Nucl. Sci. Tech. 33 (1996) 815.
[15] K. Kobayashi, G. Jin, S. Yamamoto, K. Takami, Y. Kimura, T. Kozuka, and Y. Fujita, Annu. Rep. Res. Reactor Inst., Kyoto Univ. 22 (1987) 142.
[16] S. F. Mughabghab, M. Divadeenam, and N. E. Holden, "Neutron Cross Sections", Neutron Resonance Parameters and Thermal Cross Sections, Vol. 1, part A: Z=1-60, Academic Press, New York (1984).
[17] IAEA Technical Series No. 227, Nuclear Data Standards for Nuclear Measurement, IAEA, Vienna (1983).
[18] H. W. Schmitt, ORNL-2883, 1-28-60 (1960).
[19] F. J. Briesmeister (Ed.), MCNP-A General Monte Carlo Code for Neutron and Photon Transport, Version 4B, LA-12625-M, Los Alamos National Laboratory (1997).
[20] S. Yamamoto, Y. Fujita, T. Shibata, and S. Selvi, Nucl. Instrum. Methods Phys Res. A249 (1986) 484.
[21]. J. Yoon, Nuclear Physics in print.
[22] G. D. Hickman, Bull. American Phys. Soc. 10 (1965) 12.
[23] V. McLane et al., Neutron Cross Sections, Vol. 2, Neutron Cross Section Curves, Academic Press (1988).